doi:10.1093/brain/awl009 *Brain* (2006), **129,** 899–910

A diet-induced mouse model for glutaric aciduria type I

William J. Zinnanti,[1] Jelena Lazovic,[2] Ellen B. Wolpert,[3] David A. Antonetti,[3] Michael B. Smith,[2] James R. Connor,[1] Michael Woontner,[7] Stephen I. Goodman[7] and Keith C. Cheng[4,5,6]

[1]Department of Neurosurgery, [2]Department of Radiology, Center for NMR Research, [3]Department of Cellular and Molecular Physiology and Ophthalmology, Penn State College of Medicine, [4]Department of Pathology, [5]Department of Biochemistry and Molecular Biology, [6]Department of Pharmacology, Jake Gittlen Cancer Research Foundation, Hershey, PA and [7]Department of Pediatrics, University of Colorado Health Sciences Center, Denver, CO, USA

Correspondence to: Keith C. Cheng, Jake Gittlen Cancer Research Foundation, Penn State College of Medicine, 500 University Drive, Hershey, PA 17033, USA
E-mail: kcheng@psu.edu

In the autosomal recessive human disease, glutaric aciduria type I (GA-1), glutaryl-CoA dehydrogenase (GCDH) deficiency disrupts the mitochondrial catabolism of lysine and tryptophan. Affected individuals accumulate glutaric acid (GA) and 3-hydroxyglutaric acid (3-OHGA) in the serum and often suffer acute striatal injury in childhood. Prior attempts to produce selective striatal vulnerability in an animal model have been unsuccessful. We hypothesized that acute striatal injury may be induced in GCDH-deficient (*Gcdh*$^{-/-}$) mice by elevated dietary protein and lysine. Here, we show that high protein diets are lethal to 4-week-old and 8-week-old *Gcdh*$^{-/-}$ mice within 2–3 days and 7–8 days, respectively. High lysine alone resulted in vasogenic oedema and blood–brain barrier breakdown within the striatum, associated with serum and tissue GA accumulation, neuronal loss, haemorrhage, paralysis, seizures and death in 75% of 4-week-old *Gcdh*$^{-/-}$ mice after 3–12 days. In contrast, most 8-week-old *Gcdh*$^{-/-}$ mice survived on high lysine, but developed white matter lesions, reactive astrocytes and neuronal loss after 6 weeks. Thus, the *Gcdh*$^{-/-}$ mouse exposed to high protein or lysine may be a useful model of human GA-1 including developmentally dependent striatal vulnerability.

Keywords: striatum; subarachnoid haemorrhage; animal model; blood–brain barrier; encephalopathy

Abbreviations: 3-OHGA = 3-hydroxyglutaric acid; BBB = blood–brain barrier; GA = glutaric acid; GA-1 = glutaric aciduria type I; GCDH = glutaryl-CoA dehydrogenase; GFAP = glial fibrillary acidic protein; OHGA = hydroxyglutaric acid; RITC = rhodamine isothiocyanate; WT = wild-type

Received October 6, 2005. Revised December 9, 2005. Accepted December 20, 2005. Advance Access publication January 30, 2006.

Introduction

Glutaryl-CoA dehydrogenase (EC 1.3.99.7) (GCDH) activity is required for normal mitochondrial oxidation of glutaryl-CoA produced by lysine and tryptophan catabolism. Autosomal recessive inheritance of defective alleles of GCDH results in glutaric aciduria type I (GA-1) and a loss of normal breakdown of glutaryl-CoA detected as accumulation of glutaric acid (GA), 3-hydroxyglutaric acid (3-OHGA) and glutaryl-carnitine in tissue, plasma and urine (Goodman and Frerman, 1995; Kolker *et al.*, 2003; Strauss *et al.*, 2003; Funk *et al.*, 2005).

The most striking feature of GA-1 is bilateral striatal degeneration of acute or chronic onset associated clinically with severe disabling dystonia and choreoathetosis. Histopathological findings include neuronal loss and astrogliosis in the striatum, subdural haemorrhages and spongiform vacuolation of the white matter (Goodman *et al.*, 1977; Leibel *et al.*, 1980; Chow *et al.*, 1988; Bergman *et al.*, 1989; Soffer *et al.*, 1992; Kimura *et al.*, 1994). Currently accepted therapy for GA-1 employs dietary lysine restriction through low protein diets to reduce GA-producing substrates and carnitine supplementation to prevent carnitine deficiency (Baric *et al.*, 1998). Unfortunately, about one third of children with GA-1 suffer striatal degeneration regardless of adherence to therapy (Strauss and Morton, 2003). Design of more effective therapies aimed at protecting all affected children will require a better understanding of GA-1 pathophysiology.

A GCDH-deficient mouse was generated in order to study the pathophysiology of GA-1 (Koeller *et al.*, 2002). The

GCDH knockout mouse ($Gcdh^{-/-}$) accumulates GA and 3-OHGA in serum, urine and tissue, similar to the human disease. Behavioural testing of these mice revealed mild motor deficits in otherwise healthy animals. The $Gcdh^{-/-}$ mice have not been shown to develop striatal degeneration typical of the human disease, either spontaneously or after application of metabolic or infectious stressors thought to trigger acute striatal injury (Koeller *et al.*, 2002). Adult $Gcdh^{-/-}$ mice develop vacuolation primarily in the frontal cortex.

The rationale for lysine and protein restriction as therapy for GA-1 is based on the hypothesis that the accumulation of downstream metabolites is responsible for the pathogenesis of the disease. We asked if increased dietary protein, lysine or tryptophan would aggravate disease presentation in the $Gcdh^{-/-}$ mouse. In the present study we report neuropathological, biochemical and magnetic resonance imaging changes that are associated with developmentally dependent lethality and neuropathology induced by high protein or lysine diets.

Materials and methods

Materials

All chemicals were purchased from Sigma (St Louis, MO, USA) unless otherwise specified. 3-OHGA was prepared from the dimethyl ester precursor as previously described (Cohen and Khedouri, 1960). The concentration was confirmed by gas chromatography/mass spectroscopy with a deuterated internal standard.

Animals

$Gcdh^{-/-}$ mice and wild-type (WT) littermate controls, both of mixed C57Bl/6J × 129SvEv background (Koeller *et al.*, 2002), were generated from heterozygotes and maintained at Penn State College of Medicine (Department of Comparative Medicine) in accordance with IACUC research guidelines set forth by Pennsylvania State University and the Society for Neuroscience Policy on the use of animals in neuroscience research. Male and female WT and $Gcdh^{-/-}$ mice from F1 and F2 generations were placed on special diets as 4-week-old weanlings (youngest available age to wean and place on special diets) or 8-week-old adults. Mice were sacrificed when they exhibited symptoms such as paralysis and seizures, or after 6 weeks. Mice were anaesthetized with 100 mg/kg pentobarbital (i.p.), perfused with lactate Ringer's followed by 4% paraformaldehyde for 15 min. Brains were removed and post-fixed for 48 h, and paraffin embedded.

To test blood–brain barrier (BBB) integrity, 4-week-old WT and $Gcdh^{-/-}$ mice were exposed to either normal or high lysine diets for 3 days ($n = 3$ each group). The mice were then perfused transcardially with 200 ml of 0.5% Evans blue in phosphate-buffered saline (PBS) with 500 units of heparin as previously described (Reynolds and Morton, 1998). Brains were removed and fixed for 48 h prior to dissection.

Special diets

All diets were purchased from Harland Teklad (Indianapolis, IN, USA). The high protein diet (TD.03637) (70% casein) contains 62%, rather than the 18% protein of standard diets (Harland Teklad 2018 rodent diet). This high protein diet is 4.7% lysine and 0.7% tryptophan. The high lysine diet (TD.04412) was prepared by adding free lysine to a standard diet to achieve 4.7% total lysine (5-fold of the normal diet). The high tryptophan diet (TD.04411) was prepared by adding free tryptophan to achieve 1.5% total tryptophan (7.5-fold normal). These lysine and tryptophan levels are below those previously shown to cause adverse effects in normal animals (Benevenga and Steele, 1984; Tsubuku *et al.*, 2004).

Behavioural evaluation

All special diet treated animals and corresponding controls were evaluated for motor deficits using a quantitative neurological scale developed previously (Ouary *et al.*, 2000). Motor abnormalities were scored on the presence and severity of motor symptoms consisting of dystonia (intermittent dystonia of one hindlimb, score = 1; intermittent dystonia of two hindlimbs, score = 2; permanent dystonia of hindlimbs, score = 3), gait abnormalities consisting mainly of uncoordinated, wobbling gait (score = 1), recumbency (animals lying on one side and showing uncoordinated movements when stimulated, score = 5; near death recumbency characterized by almost complete paralysis with rapid breathing, score = 6). In addition, the capability of the animals to grasp, for a few seconds, a cage grid with their forepaws (able = 0; unable = 1) and their hindpaws (able = 0; unable = 1) was assessed. The presence of these motor abnormalities was studied on a daily basis and a neurological score was calculated for each animal as the sum of all indices (minimum = 0, normal animal; maximum = 8, animal showing near death recumbency). Body temperature was measured rectally using a SAII temperature monitor (SA Instruments, Stony Brook, NY, USA). Dehydration was evaluated by weight and skin redundancy. Animals that lost 20% of their body weight within two days and exhibited skin redundancy were considered dehydrated.

Biochemical analysis

Amino acids

Serum amino acids were separated and quantified as previously described (Morton *et al.*, 2002) using a Hewlett-Packard (Palo Alto, CA, USA) 1090 series II HPLC and an Amino Quant column containing ODS-Hypersil.

Organic acids

Deuterated internal standards for GA (d4-GA) (0.0092 μmol) and 3-OHGA (d5-HGA) (0.0023 μmol) were added to 80–120 mg of brain tissue or to 20 μl of serum. Brain tissue was homogenized in 100 μl of 10 N NaOH (pH >10) and heated for 30 min at 80°C. A single 1 ml ethyl acetate extraction was used to remove cholesterol and neutral lipids. Saturated salt solution (200 μl) and 28% HCl (100 μl) were added to the remaining aqueous phase. The brain samples were extracted in 1 ml of methylene chloride to remove long-chain fatty acids and phospholipids. Serum and brain samples were extracted into 3 ml of ethyl acetate, dried under nitrogen and derivatized with 100 μl of BTSFA at 80°C for 20 min. Samples were diluted with 100 μl of ethyl acetate and 1 μl was injected onto a Hewlett-Packard 6890 gas chromatograph with a Hewlett-Packard 5973 mass spectrometer. The mass spectrometer measured total ion current for selected ions 158 and 261 (GA), 349 and 185 (3-OHGA), 265 (d4-GA), and 354 (d5-HGA) over appropriate retention times.

Liver enzyme tests

Aspartate aminotransferase (AST) and alanine aminotransferase (ALT) analyses were performed by the Department of Comparative Medicine using a CX7 Synchron automated analyser (Beckman Instruments, Fullerton, CA, USA).

MRI

MRI was performed on a 3.0 T Medspec S300 (Bruker Instruments, Ettlingen, Germany) using a 2.5 cm slotted tube resonator. MR images were obtained from 4-week-old (n = 9) and 8-week-old (n = 5) *Gcdh*$^{-/-}$ mice, and 4-week-old WT (n = 3) prior to and 3–5 days following high lysine diet exposure as they developed symptoms (hypothermia, hypoactivity, paralysis and seizures). After the baseline scan, *Gcdh*$^{-/-}$ mice on the high lysine diet were imaged once they appeared hypoactive (neurological score $\geq$ 3) and 1–3 additional times depending on survival with at least 48 h between scans. WT 4-week-old mice did not have any apparent behavioural deficits and were imaged after 3 weeks of high lysine exposure. Adult (8-week-old) *Gcdh*$^{-/-}$ mice remained asymptomatic and were imaged after 6 weeks of high lysine, and sacrificed afterwards. Prior to imaging, mice were anaesthetized with 2 mg/kg xylazine and 15 mg/kg ketamine (i.p.). Each animal was imaged with a T_2-weighted multi-echo spin echo sequence (ten 0.5 mm thick slices, TR/TE = 3000/10–152 ms, 15 echoes, 156 × 78 μm^2 resolution, 2 averages) and diffusion-weighted imaging (four 1 mm thick slices, 0.5 mm slice separation, TR/TE = 1500/70 ms, Δ = 30 ms, δ = 16 ms, b-value = 1030, 208 × 208 μm^2 resolution, 1 average, 288 s total imaging time). Transverse relaxation time constant (T_2) was calculated on a pixel-by-pixel basis from the exponential fit using CCHIPS software (Schmithorst *et al.*, 2001). Calculated T_2-values are displayed as colour-coded map. Following imaging, mice were kept at 37°C for 1 h and allowed to recover.

Histology

H&E slides were prepared from WT and *Gcdh*$^{-/-}$ mice 4–6 weeks and 12–14 weeks of age on normal or high lysine diets. Three animals were used from each group. Coronal 10 μm thick brain slices were made within 0.5 mm of the bregma line for striatal sections and between bregma −1.5 and −2.0 for hippocampal sections.

Immunohistochemistry

Glial fibrillary acidic protein (GFAP) and neuron-specific nuclear protein (NeuN) were detected using deparaffinized 10 μm thick coronal brain slices. Tissue was blocked with normal serum and incubated with polyclonal α-GFAP (1:500) (Dako, Carpenteria, CA, USA) or monoclonal α-NeuN (1:20) (Chemicon, Temecula, CA, USA) in PBS overnight at 4°C. The slides were washed three times in PBS and processed further using Vectastain ABC kits (Vector Labs, Burlingame, CA, USA) for α-rabbit (GFAP) or α-mouse (NeuN) as per the manufacturer's instructions and developed with DAB. GFAP slides were counterstained with cresyl-violet.

Neuron counts

Neurons were counted under 10× magnification of 10 μm thick sections stained for NeuN as described above. Coronal sections at bregma zero were used from *Gcdh*$^{-/-}$ normal diet controls (n = 3), lysine treated for 3 days at 4 weeks of age (n = 5), and lysine treated for 6 weeks at 8 weeks of age (n = 5). Brain areas were determined according to 'The Mouse Brain in Stereotaxic Coordinates' (Franklin and Paxinos, 1997). For cortex a 500 μm × 600 μm rectangular area from each hemisphere was selected 2 mm lateral to the mid-line with the top edge parallel to the cortical surface and extending ventral to encompass each cortical layer. For striatum a 500 μm × 600 μm rectangular area from each hemisphere was selected between 2–3 mm from the mid-line and 2–3 mm from the base of the brain. Neurons were considered NeuN positive cells with identifiable nuclei.

Striatal/cortical microvessel cultures

Rat brain microvessels were isolated as previously described (Antonetti and Wolpert, 2003) with some modifications. Male Sprague-Dawley rats (n = 11) (Taconic, Germantown, NY, USA) were anaesthetized to remove brains. Striatal and cortical parts were pooled separately after removing meninges and the choroid plexus. Tissue was Dounce-homogenized in Dulbecco's modified Eagles's medium (DMEM) (Gibco, Rockville, MD, USA) and passed over nylon mesh. The mesh fraction was washed with DMEM and collected. Separate striatal and cortical fractions were grown in MCDB-131 media supplemented with 10% foetal bovine serum, 10 ng/ml epidermal growth factor, 0.2 mg/ml ENDO GRO (VEC Technologies, Inc., Rensselaer, NY, USA), 0.09 mg/ml heparin, and antibiotic/antimycotic (Gibco, Rockville, MD, USA). Cultures were grown in a humidified incubator at 37°C under air/CO_2. Monolayer cultures were assessed for morphology by light microscopy and expression of ZO-1 (endothelial cell marker) by western blotting (data not shown).

Striatal/cortical microvessel permeability

Second and third passage striatal or cortical microvessel cultures were used to make monolayer cultures in 10.5 mm PET transwell filter plates with a 0.4 μm pore size (Becton-Dickinson, Franklin Lakes, NJ, USA) as previously described (Antonetti and Wolpert, 2003). Monolayers were confluent by the second day. GA or 3-OHGA was added at 3300 μM each. After one hour 10 μM 70 kDa rhodamine isothiocyanate (RITC)-dextran was added to the apical chamber and 100 μl aliquots were removed from the basolateral chamber at 15, 30, 45 and 60 min. The aliquots were quantified on a Fluorimager 595 (Molecular Dynamics) and P_0 values (diffusive permeability) were calculated as previously described (Chang *et al.*, 2000).

Cell viability

MTT [3-(4,5-dimethylthiazol-2-yl)-2,5-diphenyl-2-H-tetrazolium bromide] reduction (Roche Molecular Biochemicals, Indianapolis, IN, USA) was used to assess differences in cell viability of striatal or cortical monolayer cultures used in the RITC-dextran flux assays after 6 h of continued treatment.

Statistics

Normally distributed datasets were analysed by ANOVA with Fisher LSD *post hoc* test. Kruskal–Wallis one-way analysis of variance on ranks was performed with Student-Newman-Keuls *post hoc* test on samples that were not normally distributed. Sigma Stat software (Jandel Scientific, San Rafael, CA, USA) was used for analysis. A P-value < 0.05 was considered statistically significant.

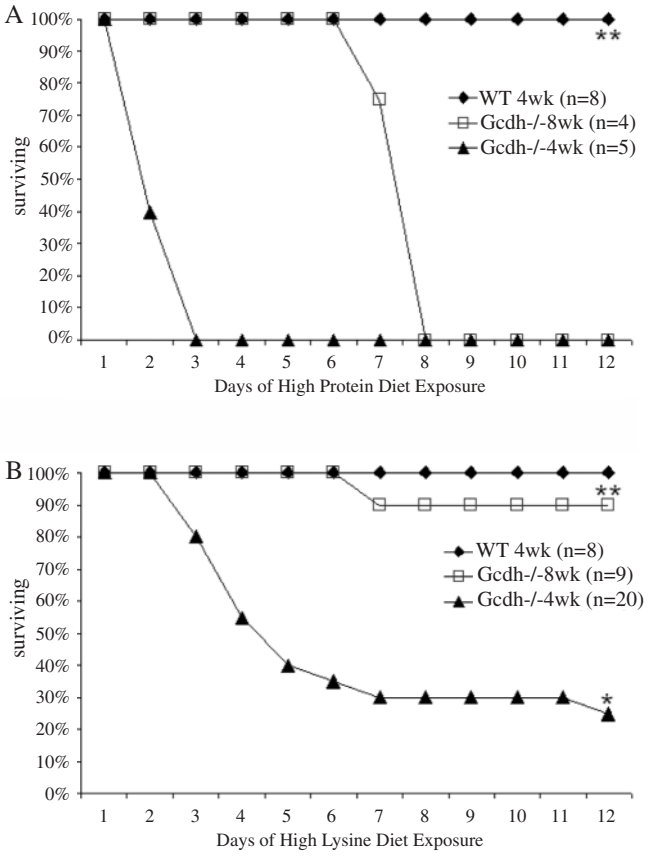

Fig. 1 Survival on special diets. Survival of (filled diamond) 4-week-old WT, (open square) 8-week-old *Gcdh*$^{-/-}$ and (filled triangle) 4-week-old *Gcdh*$^{-/-}$ mice on (**A**) 70% casein (62% protein) or (**B**) high lysine diets reveals that the high protein diet was more lethal than high lysine alone. An ability to survive the high lysine diet was observed in 25% of 4-week-old and 90% of 8-week-old *Gcdh*$^{-/-}$ mice. **Gcdh*$^{-/-}$ mouse with bilateral striatal injury after 12 days of high lysine. **WT and *Gcdh*$^{-/-}$ survivors were maintained on special diets >90 days.

Results

Survival with special diets

High protein was lethal to all *Gcdh*$^{-/-}$ mice (Fig. 1A). All 4-week-old *Gcdh*$^{-/-}$ mice died within 2–3 days of high protein diet exposure and 8-week-old *Gcdh*$^{-/-}$ mice survived slightly longer, all dying after 7–8 days. WT animals appeared normal through the 90-day test period of high protein diet exposure (Fig. 1A).

Exposure to a high lysine diet had lethal consequences for 15 of 20 (75%) 4-week-old *Gcdh*$^{-/-}$ mice, while only 1 of 9 (11%) 8-week-old *Gcdh*$^{-/-}$ mouse died following 7 days of the same high lysine diet (Fig. 1B). The remaining *Gcdh*$^{-/-}$ mice in both age groups and all isogenic WT controls survived longer than 90 days on high lysine. All *Gcdh*$^{-/-}$ and WT mice in either age group survived and remained asymptomatic on high tryptophan longer than 90 days (data not shown).

Gcdh$^{-/-}$ mice that eventually died from high protein or high lysine as well as some that survived high lysine were the only ones to manifest obvious symptoms of toxicity. For 4-week-old *Gcdh*$^{-/-}$ mice on the high lysine diet, the onset of symptoms varied 1–2 days, with a common pattern of progression: within 2–4 days of starting the diet, *Gcdh*$^{-/-}$ mice became hypothermic (28–32°C $n = 8$, 32–34°C $n = 4$); after 2 more days, mice became dehydrated and hypoactive (neurological score ≤ 3), followed by paralysis and seizures within 24 h (neurological score > 5), followed in turn by death within 12 h. Attempts to hydrate some of these animals with subcutaneous saline injections did not alter the course of symptoms or death. Two of the five surviving 4-week-old *Gcdh*$^{-/-}$ mice on high lysine became hypothermic and dehydrated, but never exhibited abnormal movements or paralysis and eventually recovered. No *Gcdh*$^{-/-}$ or WT mice exhibited symptoms with high tryptophan or normal diets.

Biochemical analysis with special diets

Serum GA levels in 4-week-old *Gcdh*$^{-/-}$ mice on a normal diet were 150 ± 5 μM (mean ± SEM). The high lysine diet raised serum GA to 2481 ± 219 μM (mean ± SEM) only in animals that displayed severe symptoms (paralysis and seizures). Asymptomatic animals maintained serum GA levels of 269 ± 48 μM (mean ± SEM), which was 80% higher than *Gcdh*$^{-/-}$ mice on a normal diet (Fig. 2A). Organic acid analysis of brain tissue from 4-week-old *Gcdh*$^{-/-}$ mice fed high lysine revealed GA levels of 3267 ± 985 μmol/kg wet weight (mean ± SEM) only in animals that had severe symptoms. *Gcdh*$^{-/-}$ mice that remained asymptomatic on high lysine had brain GA levels of 641 ± 171 μmol/kg wet weight (mean ± SEM), which was a 68% increase over 385 ± 113 μmol/kg wet weight (mean ± SEM) found in *Gcdh*$^{-/-}$ mice on the normal diet (Fig. 2B). No significant accumulation of 3-OHGA was found in serum or brain samples from *Gcdh*$^{-/-}$ mice exposed to the high lysine diet (data not shown).

Asymptomatic and symptomatic *Gcdh*$^{-/-}$ mice as well as all WT mice had significant ($P < 0.03$) serum lysine accumulation of 1257 ± 240 μM (mean ± SEM) after being placed on the high lysine diet, compared with mice on normal or tryptophan diets with serum lysine of 609 ± 187 μM (mean ± SEM) (Fig. 2C). Serum lysine of normal rodents is 245 μM (Smith, 2000). There was no difference in serum lysine accumulation between WT, symptomatic and asymptomatic *Gcdh*$^{-/-}$ mice on high lysine; therefore unlike GA accumulation, serum lysine accumulation did not correlate with disease. Symptomatic *Gcdh*$^{-/-}$ mice on the high lysine diet did have serum branched chain amino acid accumulation. Leucine, valine and isoleucine serum concentrations were significantly elevated (888 ± 3 μM, 925 ± 50 μM and 323 ± 7 μM; mean ± SEM) in the symptomatic *Gcdh*$^{-/-}$ mice placed on the high lysine diet at 4 weeks of age (Fig. 2D). In normal mice, serum leucine, valine and isoleucine concentrations are 164, 222 and 103 μM, respectively (de Boer *et al.*, 2002). AST values were slightly elevated in symptomatic *Gcdh*$^{-/-}$ mice (519 ± 12 mean ± SEM) compared with asymptomatic *Gcdh*$^{-/-}$ mice

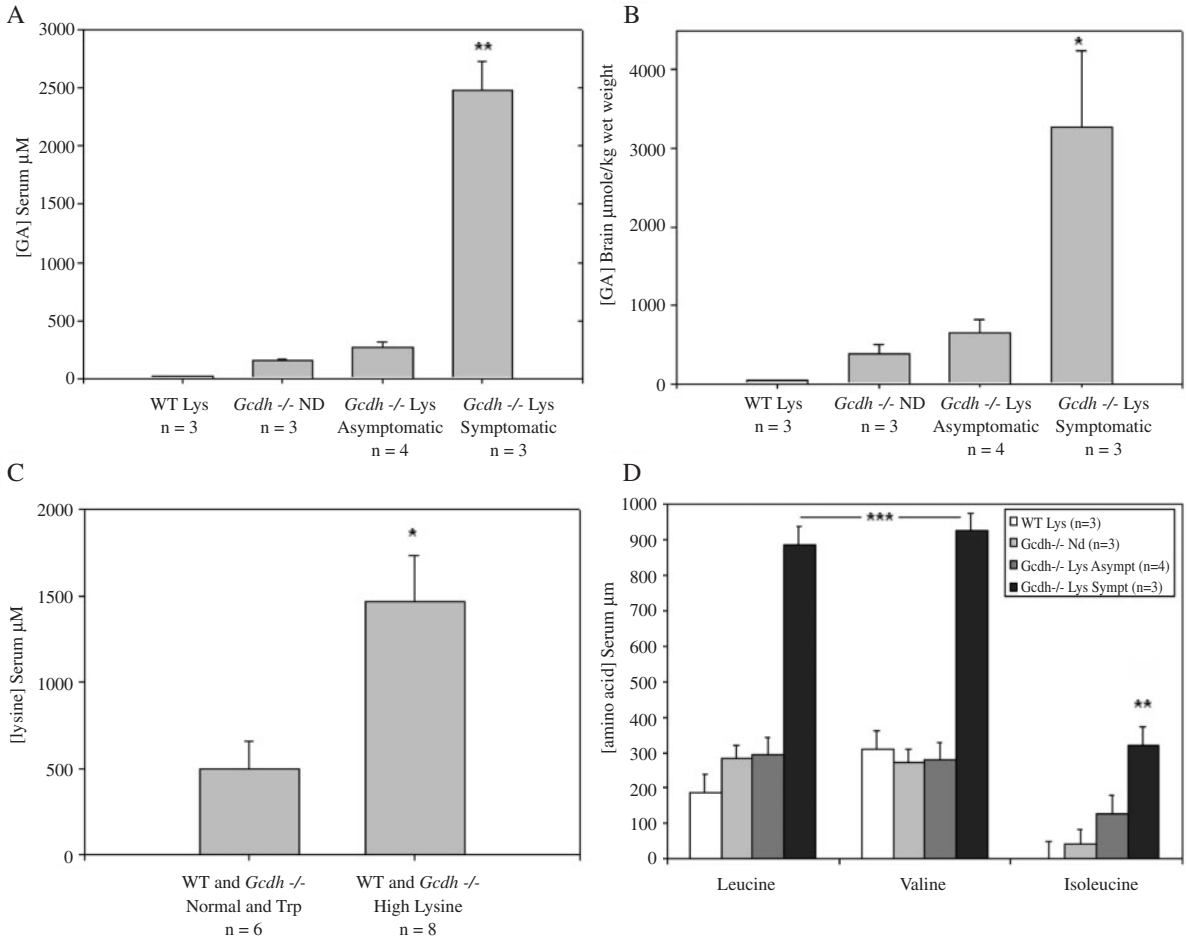

Fig. 2 Serum and brain organic acids and serum amino acid levels. (**A**) Serum and (**B**) brain glutaric acid levels (mean ± SEM) of high lysine fed WT mice (WT Lys), normal diet fed *Gcdh*$^{-/-}$ mice (*Gcdh*$^{-/-}$ ND), high lysine fed asymptomatic (*Gcdh*$^{-/-}$ Lys asymptomatic) and high lysine fed symptomatic (*Gcdh*$^{-/-}$ Lys symptomatic) *Gcdh*$^{-/-}$ mice revealed significantly increased glutaric acid levels in serum (**$P < 0.01$) and brain (*$P < 0.04$) of only symptomatic *Gcdh*$^{-/-}$ mice on high lysine. (**C**) Serum lysine levels (mean ± SEM) of high lysine fed animals indicate that WT and *Gcdh*$^{-/-}$ mice, regardless of symptoms, all accumulate significant (*$P < 0.03$) serum lysine compared with normal and high tryptophan diet fed animals. (**D**) Serum leucine, valine and isoleucine levels (mean ± SEM) for the same groups as in A and B show a significant increase (***$P < 0.001$ leucine and valine) (**$P < 0.01$ isloleucine) in serum levels for only symptomatic *Gcdh*$^{-/-}$ mice on the high lysine diet.

(309 ± 34 mean ± SEM) on the high lysine diet. There were no significant elevations or differences for ALT values and there was no obvious liver pathology (data not shown). There were no other significant correlations between diet and amino acid accumulation in the serum, including tryptophan (data not shown).

MRI

MRI findings were normal for all WT mice 3 weeks following high lysine exposure (Fig. 3A). In contrast, all symptomatic *Gcdh*$^{-/-}$ mice exhibited loss of cerebral ventricles and signal hyperintensity in deep cortical laminae and striatum on diffusion-weighted and T_2-weighted images 5–9 days after high lysine exposure (Fig. 3B). Three *Gcdh*$^{-/-}$ mice that were symptomatic after 10 days of high lysine had elevated T_2-values in the cortex and elevated T_2-values in the striatum compared with WT ($P < 0.02$) (Table 1). MRI of a symptomatic *Gcdh*$^{-/-}$ mouse with paralysis revealed bilateral striatal injury evidenced by highly elevated T_2-values (~105 ms) and diffusion-weighted signal hyperintensity in the striatum, deep cortical laminae and lateral hypothalamus after 12 days of high lysine diet exposure started at 4 weeks of age (Fig. 3C). Acute haemorrhage was present in this and three other *Gcdh*$^{-/-}$ mice prior to death (Fig. 3C, red arrow). Adult (8-week-old) *Gcdh*$^{-/-}$ mice were imaged prior to and 6 weeks following exposure to the high lysine diet. All 8-week-old *Gcdh*$^{-/-}$ mice developed bilateral signal hyperintensity in the caudate/putamen (Fig. 3D), with significantly increased T_2-values in the striatum and cortex compared with WT ($P < 0.001$) (Table 1). No abnormalities were found in *Gcdh*$^{-/-}$ mice on normal diets for up to 6 weeks.

Neuropathology

Gross dissection of brains from 4-week-old *Gcdh*$^{-/-}$ mice on high protein or lysine for 3–6 days revealed global vascular congestion and subarachnoid, subdural and intraventricular

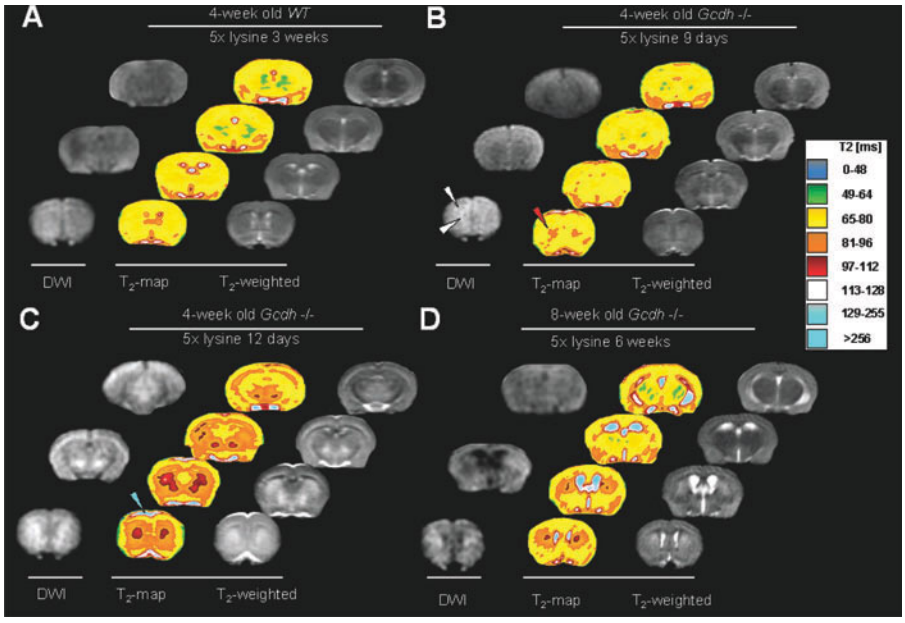

Fig. 3 MRI findings. (**A**) Normal MRI findings in a WT animal on high lysine. (**B**) *Gcdh*$^{-/-}$ mice on the high lysine diet for 9 days. Increased signal intensity on diffusion-weighted images in the cortex and striatum (white arrowheads), loss of lateral ventricles, increased T_2-values in the striatum (red arrowhead). (**C**) Striatal injury in 4-week-old *Gcdh*$^{-/-}$ mouse with paralysis after 12 days on the high lysine diet. Increased signal on diffusion and T_2-weighted images is present in the cortex and the striatum with high symmetry between two hemispheres. Matching T_2-values were highly elevated (up to 110 ms). Notice increased fluid accumulation on the top and the base of the brain (blue arrowhead), possibly resulting from subdural haemorrhage(s). (**D**) Increased signal intensity in the striatum on diffusion and T_2-weighted images in 8-week-old *Gcdh*$^{-/-}$ mouse after 6 weeks on high lysine diet. Colour scale represents different T_2-values.

Table 1 T_2-values in the cortex and in the striatum

Animal type and the diet	T_2-values (ms)	
	Cortex	Striatum
WT, 4-week old on high lysine for 3 weeks (n = 3)	72.27 ± 0.72	73.2 ± 0.62
Gcdh$^{-/-}$, 4-week old on normal diet (n = 3)	73.07 ± 0.96	74.23 ± 1.86
Gcdh$^{-/-}$, 4-week old on high lysine for 10 days (n = 3)	76.4 ± 2.72	82.33 ± 2.41*†
Gcdh$^{-/-}$, 8-week old on high lysine for 6 weeks (n = 3)	77.07 ± 0.29*†	88.47 ± 1.65*†

Values are mean ± SD. *P < 0.001 versus WT. †P < 0.02 versus *Gcdh*$^{-/-}$ on normal diet.

haemorrhages (Fig. 4). No obvious thrombus or other obstructions were found within the congested vessels of this group.

Microscopic examination of brains from *Gcdh*$^{-/-}$ mice on high lysine confirmed the ventricular obliteration shown by MRI (Fig. 5, middle). Higher magnification of the cortex and striatum revealed large irregular vacuoles and dilation of the capillary bed compared with normal diet fed animals (Fig. 5, left). *Gcdh*$^{-/-}$ mice on a normal diet had moderate vacuolation in the cortex that was less severe in the striatum, as previously reported (Koeller *et al.*, 2002) (Fig. 5, left). *Gcdh*$^{-/-}$ mice surviving on high lysine for 6 weeks showed severe vacuolation of the white matter patches of the striatum bilaterally (Fig. 5, right). Moderately increased vacuolation was also found in the deeper laminae of the cortex. This pattern of increased vacuolation correlated with the location of elevated T_2-values in these animals (compare Fig. 5, right, with Fig. 3D). There were no differences observed between WT animals on high lysine and normal diets.

Neuronal loss

Severe disruption of cortical architecture with neuronal loss, confirmed by NeuN positive cell counts, was found in *Gcdh*$^{-/-}$ mice exposed to high lysine for 3 days (Fig. 6). *Gcdh*$^{-/-}$ mice exposed to high lysine at 8 weeks of age for 6 weeks showed neuronal loss in the cortex and striatum, confirmed by NeuN positive cell counts, and severe vacuolation of striatal patches (Fig. 6).

Gliosis

GFAP staining of brains from 8-week-old *Gcdh*$^{-/-}$ mice on the high lysine diet for 6 weeks revealed gliosis of the cortex

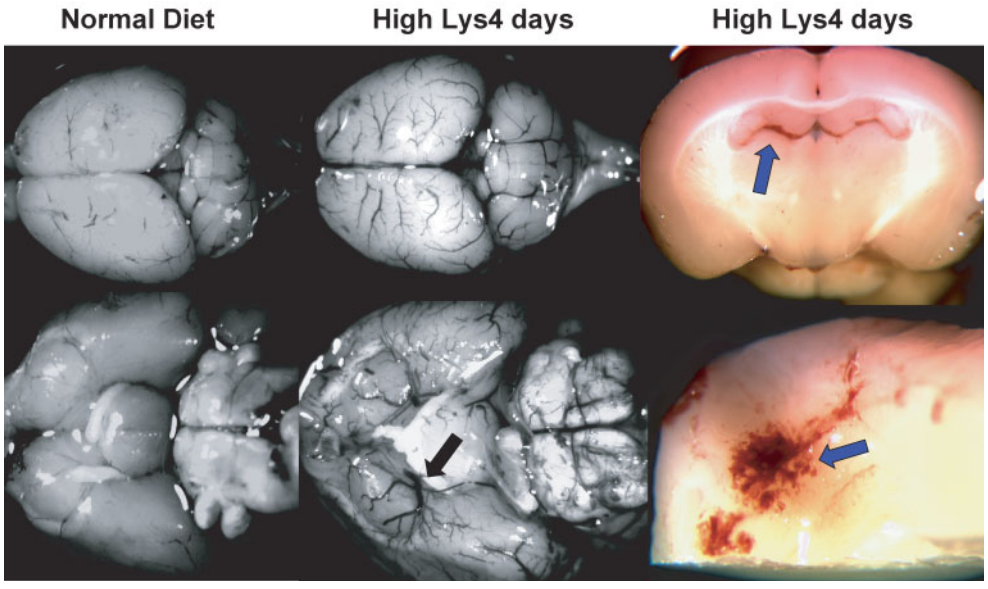

Fig. 4 Gross pathology. Comparison of 4-week-old *Gcdh*$^{-/-}$ mouse brains after 4 days of normal diet (left) or high lysine (middle and right) reveals engorged blood vessels and subarachnoid haemorrhage on gross examination. Note large engorged branching vein (black arrow, lower middle) at the right middle cerebral artery branch point of the circle of Willis. Coronal section of a 4-week-old *Gcdh*$^{-/-}$ mouse brain (upper right) after 4 days of high lysine diet reveals subarachnoid haemorrhage (blue arrow) dissecting below the hippocampus bilaterally. With the cortex inverted and thalamus dissected away, the haemorrhage is traced to the choroidal branch of the posterior cerebral artery (blue arrow, lower right).

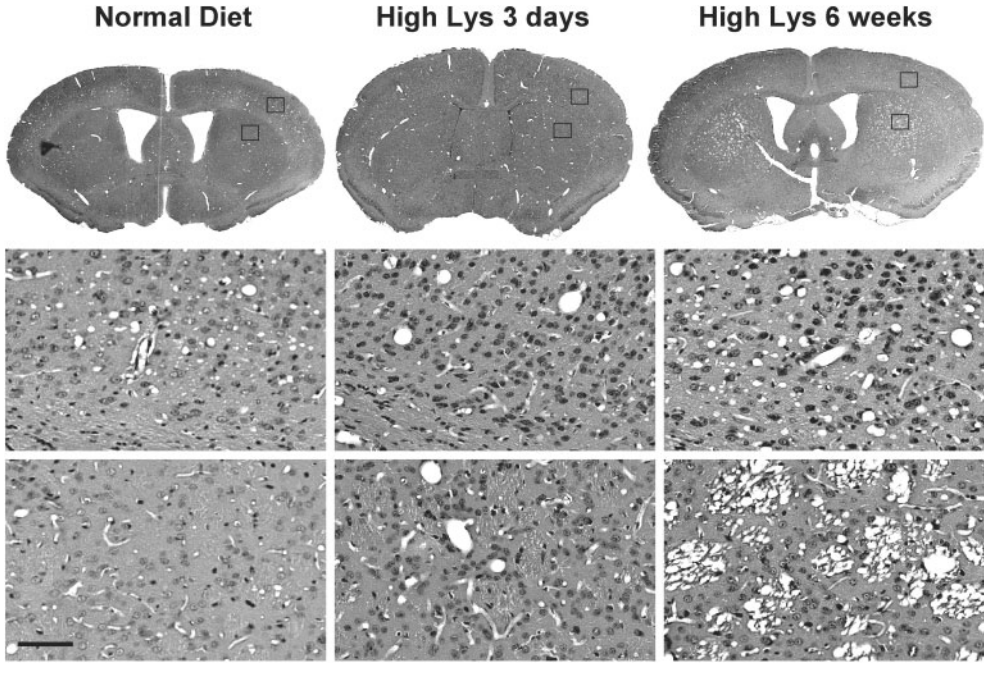

Fig. 5 Microscopic pathology. Comparison of H&E brain sections from *Gcdh*$^{-/-}$ mice maintained on normal diet, high lysine for 3 days starting at 4 weeks of age, or high lysine for 6 weeks starting at 8 weeks of age. Whole coronal sections (*top* row) are shown with boxes indicating location of corresponding higher magnified cortex (*middle* row) and striatum (*bottom* row). Compared with normal (*top* row, left), high lysine for 3 days at 4 weeks of age revealed a swollen brain with loss of normal contrast between cortex and striatum and obliterated ventricles (*top* row, middle). Intense vacuolation bilaterally in the striatum was noted after 6 weeks of high lysine exposure beginning at 8 weeks of age (*top* right). Higher magnification of the cortex and striatum (*middle* and *bottom* row) shows large irregular vacuoles and capillary distension after 3 days of lysine exposure (*middle*) compared with normal (left). Increased vacuolation of the cortex and severe vacuolation of the white matter patches were found after 6 weeks of high lysine exposure (*middle* and *bottom* row, right). (All images H&E, 5× top row, 100× middle and bottom rows, Bar = 100 μm middle and bottom row).

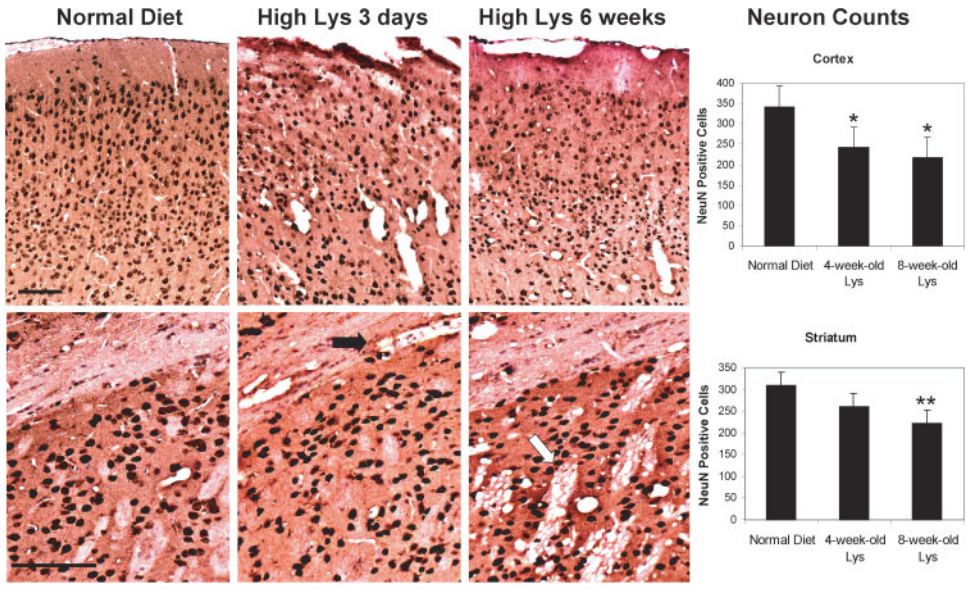

Fig. 6 Neuronal loss. NeuN stained sections from cortex (*top* row) and striatum (*bottom* row) of *Gcdh*$^{-/-}$ mice maintained on normal diet, high lysine for 3 days and high lysine for 6 weeks with associated neuron counts. Neuron staining reveals disrupted cortical architecture, neuronal loss and large irregular vacuoles in the cortex and striatum (black arrow) after 3 days of high lysine exposure compared with normal. After 6 weeks of high lysine exposure, neuronal loss is noted in the cortex and intense vacuolation invades the striatal patches (white arrow). Neuron counts reveal significant neuronal loss in the cortex (*$P < 0.05$) after 3 days and 6 weeks of lysine exposure and in the striatum (*$P < 0.002$) after lysine diet exposure for 6 weeks. (100× *top* row, 200× *bottom* row, Bar = 100 μm *top* and *bottom* rows.)

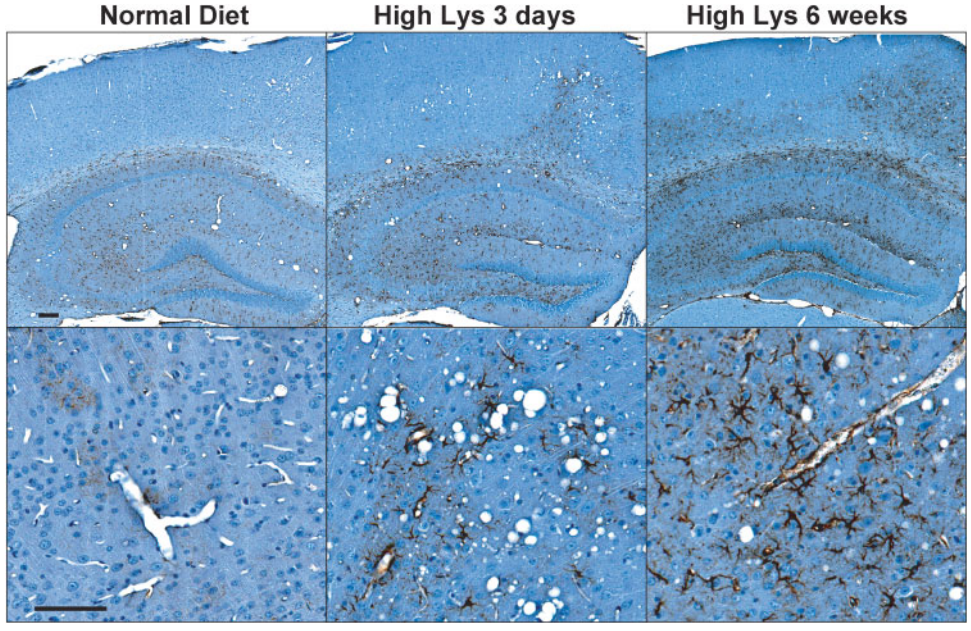

Fig. 7 Gliosis. GFAP stained sections from *Gcdh*$^{-/-}$ mice maintained on normal diet, high lysine for 3 days and high lysine for 6 weeks. *Gcdh*$^{-/-}$ mice exposed to high lysine for 3 days (*middle*) had increased numbers of reactive astrocytes compared with normal diet controls (left). *Gcdh*$^{-/-}$ mice exposed to high lysine for 6 weeks had notably intense astrocyte activation (right). Higher magnification (*bottom* row) reveals activated astrocytes located adjacent to blood vessels with end-foot thickening (*bottom*, *middle* and right). (*Top* row 20×, *bottom* row 100×, Bar = 200 μm *top* row, 100 μm *bottom* row.)

and hippocampus that was less obvious in the striatum (Fig. 7, right). The 4-week-old *Gcdh*$^{-/-}$ mice on the high lysine diet for 3 days developed some gliosis in the same areas, which was less severe compared with the 8-week-old *Gcdh*$^{-/-}$ mice exposed to lysine for 6 weeks (Fig. 7, middle). Gliosis was absent from WT and *Gcdh*$^{-/-}$ mice on a normal diet and WT mice on high lysine for 6 weeks (Fig. 7, left, WT data not shown).

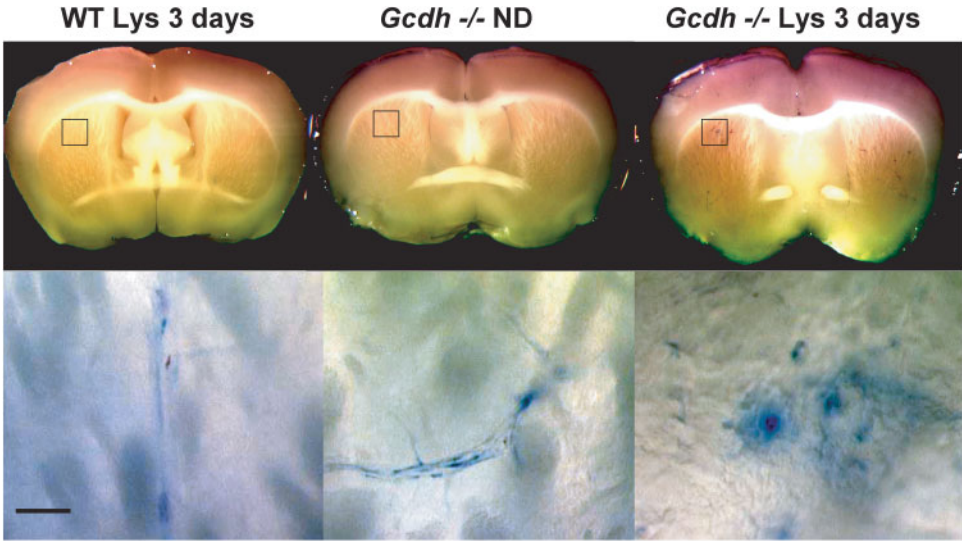

Fig. 8 Blood–brain barrier breakdown. Gross coronal sections from Evans blue perfusion of 4-week-old WT mice exposed to high lysine for 3 days, 4-week-old *Gcdh*$^{-/-}$ mice maintained on a normal diet (ND), and 4-week-old *Gcdh*$^{-/-}$ mice exposed to high lysine for 3 days. BBB breakdown is noted in the striatum of the *Gcdh*$^{-/-}$ mouse exposed to high lysine only (right). (*Top* row box indicates area of higher magnification in *bottom* row, Bar = 200 μm *bottom* row.)

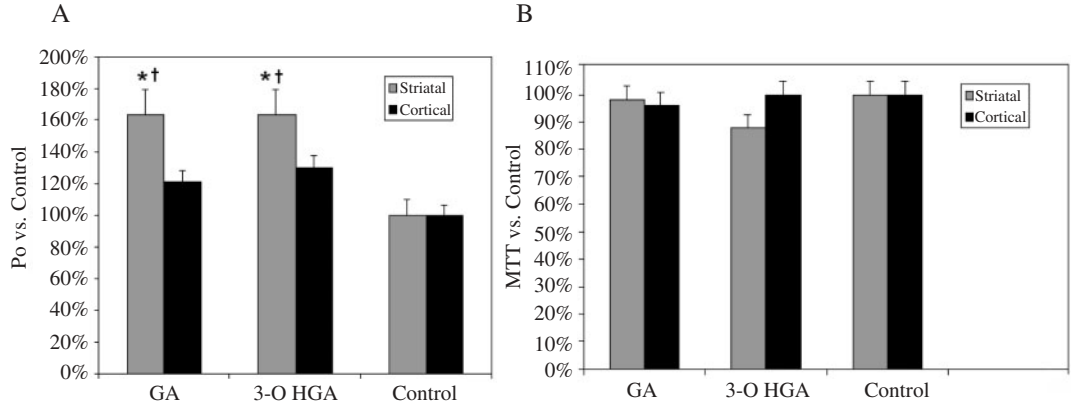

Fig. 9 Increased striatal microvessel permeability with GA or 3-OHGA. (**A**) Permeability of rat brain striatal and cortical microvessel monolayers detected as % RITC-dextran flux (Po) (mean ± SEM) after 2 h treatment without (control) or with 3300 μM GA or 3-OHGA. Striatal microvessels had significantly ($^{\dagger}P < 0.001$) increased permeability with both GA and 3-OHGA compared with controls and compared with cortical microvessels ($^{*}P < 0.03$). (**B**) Cell viability assay (mean ± SEM) reveals no significant difference after 6 h of continued treatment with GA and 3-OHGA compared with control.

Blood–brain barrier breakdown

Evans blue stain was found in the choroid plexus and circumventricular organs in all animals of each group tested. *Gcdh*$^{-/-}$ mice placed on high lysine at 4 weeks of age for 3 days showed extravasation of Evans blue in the striatum, indicating BBB breakdown. Evans blue was found to escape from smaller vessels of the striatum (Fig. 8, right). Some larger vessels in the striatum of this group had concentrated blue staining and vasodilatation consistent with congestion. These observations were absent from the cortex in this group. WT mice on high lysine and *Gcdh*$^{-/-}$ mice on a normal diet, both 4 weeks of age, showed no evidence of BBB breakdown (Fig. 8, left and middle).

Increased striatal microvessel permeability with GA and 3-OHGA

To investigate whether GA or 3-OHGA can induce breakdown of the BBB, a previously studied model (Antonetti and Wolpert, 2003) of rat striatal and cortical microvessels was isolated and permeability of monolayers to RITC-Dextran was measured. Striatal microvessels were significantly more permeable to RITC-dextran flux after treatment

with 3300 μM GA or 3-OHGA compared with cortical microvessels ($P < 0.03$) and controls ($P < 0.001$) (Fig. 9A). Increased permeability was not due to significant endothelial cell death. There were no significant differences in cell viability of monolayer cultures between any treatment groups and controls after 6 h of continued treatment (Fig. 9B).

Discussion

The lack of severe spontaneous neuropathology in *Gcdh*$^{-/-}$ mice provides an opportunity to test environmental manipulations that may trigger the neuropathology seen in human GA-1. We hypothesized that increased dietary lysine in the context of GCDH deficiency would result in increased GA accumulation and trigger neuropathology in the *Gcdh*$^{-/-}$ mouse. Here we provide the first evidence that high protein and high lysine diets can cause neuropathology and death in a mouse model of GCDH deficiency. By applying these diets to weanling and adult *Gcdh*$^{-/-}$ mice, we have uncovered developmentally dependent lysine toxicity and two distinct types of injury based on age and length of diet exposure. Weanling *Gcdh*$^{-/-}$ mice placed on high lysine at 4 weeks of age present with an acute onset of symptoms including paralysis and seizures, associated with large accumulation of GA in serum and brain. Gross and microscopic examination of brains from these mice reveal BBB breakdown in the striatum and haemorrhages. MRI examination of a paralysed young *Gcdh*$^{-/-}$ mouse on the high lysine diet revealed acute bilateral striatal damage resembling the characteristic injury of human GA-1 (Baric *et al.*, 1998; Strauss and Morton, 2003). In contrast, all the 8-week-old adult *Gcdh*$^{-/-}$ mice that survived and remained asymptomatic on high lysine for 6 weeks developed specific striatal lesions, evident as hyperintense T_2- and diffusion-weighted signals. Microscopic examination of the brains from this group revealed disruption of white matter patches resulting from intense vacuolation within the striatum. The striatal changes were accompanied by reactive astrocytes in the cortex and hippocampus and neuronal loss in the cortex and striatum. These findings are consistent with the recently described adult onset GA-1 leucodystrophy (Bahr *et al.*, 2002). The results of high lysine and protein diet exposure in young *Gcdh*$^{-/-}$ mice strongly support the use of protein and lysine restriction as standard therapy in human GA-1. Furthermore, the detrimental effects of high protein and lysine on adult *Gcdh*$^{-/-}$ mice support the suggestion that GA-1 patients maintain life-long dietary restriction (Bahr *et al.*, 2002; Kolker and Hoffmann, 2003).

Brain GA accumulation correlates with neuropathology

Brain GA levels correlated with and may be responsible for the severe neuropathology in young *Gcdh*$^{-/-}$ mice exposed to the high lysine diet. *Gcdh*$^{-/-}$ mice that developed severe symptoms of paralysis and seizures or died after high lysine exposure accumulated brain GA levels above 1600 μmol/kg wet wt (~2 mM based on 80% water content). The level was consistently below 800 μmol/kg wet wt (<1 mM) in asymptomatic mice. Symptomatic and asymptomatic *Gcdh*$^{-/-}$ mice on the high lysine diet accumulated similar concentrations of serum lysine. *Gcdh*$^{-/-}$ mice were not found to accumulate significant 3-OHGA. Therefore, GA accumulation correlates with disease and lysine accumulation does not.

Extracellular exposure versus intracellular accumulation of GA

Previous studies of GA exposure to organotypic slice cultures (Ullrich *et al.*, 1999) and immature oligodendrocytes (OLN-93 cells) (Gerstner *et al.*, 2005) provide evidence that extracellular GA exposure to immature oligodendrocytes may explain observed vacuolation seen in human GA-1 and *Gcdh*$^{-/-}$ mice. Here we provide evidence that extracellular GA exposure (3.3 mM) can disrupt BBB properties of striatal endothelial cells. Conversely, studies utilizing the extracellular approach of GA exposure to neuronal cell cultures or intrastriatal injections *in vivo* have failed to demonstrate repeatable neurotoxicity at disease relevant concentrations that can be applied as a model of neuronal loss in GA-1 (Lima *et al.*, 1998; Ullrich *et al.*, 1999; Kolker *et al.*, 2000; Funk *et al.*, 2004; Gerstner *et al.*, 2005). The neuropathology found in *Gcdh*$^{-/-}$ mice exposed to high lysine may represent the effects of intracellular GA accumulation generated from increased lysine metabolism in the context of GCDH deficiency. GA generated within cells may cause toxicity by disrupting normal cellular processes. Induction of mitochondrial permeability transition, inhibition of glutamate decarboxlyase and alpha-keto-glutarate dehydrogenase as well as glutathione depletion have all been demonstrated at GA concentrations below those found in symptomatic *Gcdh*$^{-/-}$ mice on high lysine (Stokke *et al.*, 1976; Palmeira *et al.*, 2000; Sauer *et al.*, 2005). These effects would require GA accumulation within cells or subcellular compartments. Alternatively, the process of producing GA may be toxic. Rapidly generated glutaryl-CoA from increased lysine oxidation within mitochondria may temporarily sequester limited CoA from vital citric acid cycle reactions, reducing available ATP. Accumulation of glutaryl-carnitine with carnitine depletion observed in GA-1 patients supports the hypothesis of CoA sequestration. Carnitine exchange for CoA is required to extract glutarate from mitochondria and free up the limited CoA pool (Russell *et al.*, 1995; Ramsay and Zammit, 2004). The differential toxicity between the high protein and the high lysine diet, having the same lysine content, further supports the hypothesis that the process of generating GA may be toxic. A high protein diet can induce increases in lysine oxidation. Blemings *et al.* (1998), showed that a 60% casein diet can double lysine oxidation over a 20% casein diet in rat liver homogenates (casein is 87% protein). A 70% casein diet would be expected to more than double the lysine oxidation over the high lysine diet having only 18% protein. However, we cannot rule out the possibility of a synergistic effect of

increased lysine and tryptophan together or another amino acid causing the observed severity for all *Gcdh*$^{-/-}$ mice on the high protein diet. Within the brain it remains to be shown in which cell types, in what form (GA, glutaryl-CoA, glutaryl-carnitine, glutaryl-glutathione) and how much GA accumulates as well as possible uptake, transport or excretion between cells and how production and elimination of GA are regulated.

Vascular injury

While hypotheses of neurotoxicity in GA-1 have been widely studied, they fail to demonstrate mechanisms that can parallel the rapid progression and regional specificity of acute striatal necrosis (Funk *et al.*, 2004; Kolker *et al.*, 2004; Funk *et al.*, 2005; Strauss, 2005). Vascular injury as a paradigm of pathogenesis in GA-1 has been far less explored and can account for the rapid progression of striatal necrosis. However, models of vascular injury including bilateral carotid occlusion (Canese *et al.*, 1997) or induced renal hypertension (Del Bigio *et al.*, 1999) do not show the degree of symmetry found in GA-1. Distended blood vessels, BBB breakdown and haemorrhages indicate a vascular component of this disease, as previously suggested for humans (Haworth *et al.*, 1991; Osaka *et al.*, 1993; Kimura *et al.*, 1994; Woelfle *et al.*, 1996; Hartley *et al.*, 2001; Strauss *et al.*, 2003; Muhlhausen *et al.*, 2004; Funk *et al.*, 2005). Our results reveal BBB breakdown as an early pathophysiological event for young *Gcdh*$^{-/-}$ mice exposed to the high lysine diet. Furthermore, our permeability studies support regional specificity by demonstrating a difference in the ability to maintain barrier properties between striatal and cortical derived microvessels when exposed to GA levels (3.3 mM) similar to those found in brains of *Gcdh*$^{-/-}$ mice on the high lysine diet and GA-1 patients (Funk *et al.*, 2005). Although the effect of 3-OHGA on striatal microvessels was similar, this compound has not been found at these concentrations in brain of human or mice with GCDH deficiency (Koeller *et al.*, 2002; Funk *et al.*, 2005).

Branch chain amino acid accumulation was found in serum of symptomatic *Gcdh*$^{-/-}$ mice on the high lysine diet and suggest an acute phase reaction of liver damage (Tarasow *et al.*, 2003). However, ALT levels and liver histology, of young symptomatic *Gcdh*$^{-/-}$ mice after high lysine exposure, are not comparable with a mouse model of hepatic encephalopathy (Matkowskyj *et al.*, 1999).

In conclusion, our results indicate that the *Gcdh*$^{-/-}$ mouse may indeed be a good model to study the development of neuropathology that characterizes human GA-1. Dietary protein, specifically lysine restriction, is strongly supported as standard therapy for GA-1, and life-long dietary restriction should be considered. This model may be used to further elucidate the underlying pathophysiology of this disease, which may in turn lead to effective ways of protecting children identified by newborn screening from the devastating clinical sequelae of striatal damage.

Acknowledgements

The authors dedicate this work to the memory of Dr Linda Crnic, who contributed significantly to the development of the *Gcdh* knockout mouse and also generated the mice used in this work. The authors thank Dr Kevin A. Strauss and Dr D. Holmes Morton for help with biochemistry and thoughtful guidance and suggestions in the course of their work. The authors also thank Lindsay Rush for help with preparation of figures. This work is supported by the Laverty and Oxford Foundations. M.B.S. acknowledges the support of NIH R01 EB000454.

References

Antonetti DA, Wolpert EB. Isolation and characterization of retinal endothelial cells. In: Nag S, editor. Methods in molecular medicine. Vol. 89. Totowa, NJ: Humanna Press, Inc.; 2003.

Bahr O, Mader I, Zschocke J, Dichgans J, Schulz JB. Adult onset glutaric aciduria type I presenting with a leukoencephalopathy. Neurology 2002; 59: 1802–4.

Baric I, Zschocke J, Christensen E, Duran M, Goodman SI, Leonard JV, et al. Diagnosis and management of glutaric aciduria type I. J Inherit Metab Dis 1998; 21: 326–40.

Benevenga NJ, Steele RD. Adverse effects of excessive consumption of amino acids. Annu Rev Nutr 1984; 4: 157–81.

Bergman I, Finegold D, Gartner JC Jr, Zitelli BJ, Claassen D, Scarano J, et al. Acute profound dystonia in infants with glutaric acidemia. Pediatrics 1989; 83: 228–34.

Blemings KP, Crenshaw TD, Benevenga NJ. Mitochondrial lysine uptake limits hepatic lysine oxidation in rats fed diets containing 5, 20 or 60% casein. J Nutr 1998; 128: 2427–34.

Canese R, Podo F, Fortuna S, Lorenzini P, Michalek H. Transient global brain ischemia in the rat: spatial distribution, extension, and evolution of lesions evaluated by magnetic resonance imaging. Magma 1997; 5: 139-49.

Chang YS, Munn LL, Hillsley MV, Dull RO, Yuan J, Lakshminarayanan S, et al. Effect of vascular endothelial growth factor on cultured endothelial cell monolayer transport properties. Microvasc Res 2000; 59: 265–77.

Chow CW, Haan EA, Goodman SI, Anderson RM, Evans WA, Kleinschmidt-DeMasters BK, et al. Neuropathology in glutaric acidaemia type 1. Acta Neuropathol (Berl) 1988; 76: 590–4.

Cohen SG, Khedouri E. Requirements for stereospecificity in hydrolysis by chymotrypsin: diethyl beta-acetamidoglutarate. Nature 1960; 186: 75–6.

de Boer J, Andressoo JO, de Wit J, Huijmans J, Beems RB, van Steeg H, et al. Premature aging in mice deficient in DNA repair and transcription. Science 2002; 296: 1276–9.

Del Bigio MR, Yan HJ, Kozlowski P, Sutherland GR, Peeling J. Serial magnetic resonance imaging of rat brain after induction of renal hypertension. Stroke 1999; 30: 2440–7.

Franklin KBJ, Paxinos G. The mouse brain in stereotaxic coordinates. San Diego, CA: Academic Press, Inc.; 1997.

Funk CB, Prasad AN, Del Bigio MR. Preliminary attempts to establish a rat model of striatal injury in glutaric acidaemia type I. J Inherit Metab Dis 2004; 27: 819–24.

Funk CB, Prasad AN, Frosk P, Sauer S, Kolker S, Greenberg CR, et al. Neuropathological, biochemical and molecular findings in a glutaric acidemia type 1 cohort. Brain 2005; 128: 711–22.

Gerstner B, Gratopp A, Marcinkowski M, Sifringer M, Obladen M, Buhrer C. Glutaric acid and its metabolites cause apoptosis in immature oligodendrocytes: a novel mechanism of white matter degeneration in glutaryl-CoA dehydrogenase deficiency. Pediatr Res 2005; 57: 771–6.

Goodman SI, Frerman FE. Organic acidemias due to defects in lysine oxidation: 2-ketoadipic academia and glutaric academia. In: Scriver C, Beudet A, Sly W, Valle D, editors. The metabolic and molecular bases of inherited disease. New York: McGraw Hill; 1995. p. 2195–204.

Goodman SI, Norenberg MD, Shikes RH, Breslich DJ, Moe PG. Glutaric aciduria: biochemical and morphologic considerations. J Pediatr 1977; 90: 746–50.

Hartley LM, Khwaja OS, Verity CM. Glutaric aciduria type 1 and nonaccidental head injury. Pediatrics 2001; 107: 174–5.

Haworth JC, Booth FA, Chudley AE, deGroot GW, Dilling LA, Goodman SI, et al. Phenotypic variability in glutaric aciduria type I: report of fourteen cases in five Canadian Indian kindreds. J Pediatr 1991; 118: 52–8.

Kimura S, Hara M, Nezu A, Osaka H, Yamazaki S, Saitoh K. Two cases of glutaric aciduria type 1: clinical and neuropathological findings. J Neurol Sci 1994; 123: 38–43.

Koeller DM, Woontner M, Crnic LS, Kleinschmidt-DeMasters B, Stephens J, Hunt EL, et al. Biochemical, pathologic and behavioural analysis of a mouse model of glutaric acidemia type I. Hum Mol Genet 2002; 11: 347–57.

Kolker S, Hoffmann GF. Adult onset glutaric aciduria type I presenting with a leukoencephalopathy. Neurology 2003; 60: 1399.

Kolker S, Ahlemeyer B, Krieglstein J, Hoffmann GF. Maturation-dependent neurotoxicity of 3-hydroxyglutaric and glutaric acids in vitro: a new pathophysiologic approach to glutaryl-CoA dehydrogenase deficiency. Pediatr Res 2000; 47: 495–503.

Kolker S, Hoffmann GF, Schor DS, Feyh P, Wagner L, Jeffrey I, et al. Glutaryl-CoA dehydrogenase deficiency: region-specific analysis of organic acids and acylcarnitines in post mortem brain predicts vulnerability of the putamen. Neuropediatrics 2003; 34: 253–60.

Kolker S, Strauss KA, Goodman SI, Hoffmann GF, Okun JG, Koeller DM. Challenges for basic research in glutaryl-CoA dehydrogenase deficiency. J Inherit Metab Dis 2004; 27: 843–9.

Leibel RL, Shih VE, Goodman SI, Bauman ML, McCabe ER, Zwerdling RG, et al. Glutaric acidemia: a metabolic disorder causing progressive choreoathetosis. Neurology 1980; 30: 1163–8.

Lima TT, Begnini J, de Bastiani J, Fialho DB, Jurach A, Ribeiro MC, et al. Pharmacological evidence for GABAergic and glutamatergic involvement in the convulsant and behavioral effects of glutaric acid. Brain Res 1998; 802: 55–60.

Matkowskyj KA, Marrero JA, Carroll RE, Danilkovich AV, Green RM, Benya RV. Azoxymethane-induced fulminant hepatic failure in C57BL/6J mice: characterization of a new animal model. Am J Physiol 1999; 277: G455–62.

Morton DH, Strauss KA, Robinson DL, Puffenberger EG, Kelley RI. Diagnosis and treatment of maple syrup disease: a study of 36 patients. Pediatrics 2002; 109: 999–1008.

Muhlhausen C, Ergun S, Strauss KA, Koeller DM, Crnic L, Woontner M, et al. Vascular dysfunction as an additional pathomechanism in glutaric aciduria type I. J Inherit Metab Dis 2004; 27: 829–34.

Osaka H, Kimura S, Nezu A, Yamazaki S, Saitoh K, Yamaguchi S. Chronic subdural hematoma, as an initial manifestation of glutaric aciduria type-1. Brain Dev 1993; 15: 125–7.

Ouary S, Bizat N, Altairac S, Menetrat H, Mittoux V, Conde F, et al. Major strain differences in response to chronic systemic administration of the mitochondrial toxin 3-nitropropionic acid in rats: implications for neuroprotection studies. Neuroscience 2000; 97: 521–30.

Palmeira CM, Rana MI, Frederick CB, Wallace KB. Induction of the mitochondrial permeability transition in vitro by short-chain carboxylic acids. Biochem Biophys Res Commun 2000; 272: 431–5.

Ramsay RR, Zammit VA. Carnitine acyltransferases and their influence on CoA pools in health and disease. Mol Aspects Med 2004; 25: 475–93.

Reynolds DS, Morton AJ. Changes in blood-brain barrier permeability following neurotoxic lesions of rat brain can be visualised with trypan blue. J Neurosci Methods 1998; 79: 115–21.

Russell RR 3rd, Mommessin JI, Taegtmeyer H. Propionyl-L-carnitine-mediated improvement in contractile function of rat hearts oxidizing acetoacetate. Am J Physiol 1995; 268: H441–7.

Sauer SW, Okun JG, Schwab MA, Crnic LR, Hoffmann GF, Goodman SI, et al. Bioenergetics in glutaryl-coenzyme A dehydrogenase deficiency: a role for glutaryl-coenzyme A. J Biol Chem 2005; 280: 21830–6.

Schmithorst VJ, Dardzinski BJ, Holland SK. Simultaneous correction of ghost and geometric distortion artifacts in EPI using a multiecho reference scan. IEEE Trans Med Imaging 2001; 20: 535–9.

Smith QR. Transport of glutamate and other amino acids at the blood-brain barrier. J Nutr 2000; 130: 1016S–22S.

Soffer D, Amir N, Elpeleg ON, Gomori JM, Shalev RS, Gottschalk-Sabag S. Striatal degeneration and spongy myelinopathy in glutaric acidemia. J Neurol Sci 1992; 107: 199–204.

Stokke O, Goodman SI, Moe PG. Inhibition of brain glutamate decarboxylase by glutarate, glutaconate, and beta-hydroxyglutarate: explanation of the symptoms in glutaric aciduria? Clin Chim Acta 1976; 66: 411–5.

Strauss KA. Glutaric aciduria type 1: a clinician's view of progress. Brain 2005; 128: 697–9.

Strauss KA, Morton DH. Type I glutaric aciduria, part 2: a model of acute striatal necrosis. Am J Med Genet C Semin Med Genet 2003; 121: 53–70.

Strauss KA, Puffenberger EG, Robinson DL, Morton DH. Type I glutaric aciduria, part 1: natural history of 77 patients. Am J Med Genet C Semin Med Genet 2003; 121: 38–52.

Tarasow E, Panasiuk A, Siergiejczyk L, Orzechowska-Bobkiewicz A, Lewszuk A, Walecki J, et al. MR and 1H MR spectroscopy of the brain in patients with liver cirrhosis and early stages of hepatic encephalopathy. Hepatogastroenterology 2003; 50: 2149–53.

Tsubuku S, Mochizuki M, Mawatari K, Smriga M, Kimura T. Thirteen-week oral toxicity study of L-lysine hydrochloride in rats. Int J Toxicol 2004; 23: 113–8.

Ullrich K, Flott-Rahmel B, Schluff P, Musshoff U, Das A, Lucke T, et al. Glutaric aciduria type I: pathomechanisms of neurodegeneration. J Inherit Metab Dis 1999; 22: 392–403.

Woelfle J, Kreft B, Emons D, Haverkamp F. Subdural haemorrhage as an initial sign of glutaric aciduria type 1: a diagnostic pitfall. Pediatr Radiol 1996; 26: 779–81.